BIOCHEMISTRY
including biophysical chemistry & molecular biology

Article

pubs.acs.org/biochemistry

Structural Basis Unifying Diverse GTP Hydrolysis Mechanisms

Baskaran Anand,[†] Soneya Majumdar, and Balaji Prakash*

Department of Biological Sciences and Bioengineering, Indian Institute of Technology, Kanpur 208016, India

Supporting Information

ABSTRACT: Central to biological processes is the regulation rendered by GTPases. Until recently, the GTP hydrolysis mechanism, exemplified by Ras-family (and G-α) GTPases, was thought to be universal. This mechanism utilizes a conserved catalytic Gln supplied "in *cis*" from the GTPase and an arginine finger "in *trans*" from a GAP (GTPase activating protein) to stabilize the transition state. However, intriguingly different mechanisms are operative in structurally similar GTPases. MnmE and dynamin like cation-dependent GTPases lack the catalytic Gln and instead employ a Glu/Asp/Ser situated elsewhere and in place of the arginine finger use a K^+ or Na^+ ion. In contrast, Rab33 possesses the Gln but does not utilize it for catalysis; instead, the GAP supplies both a catalytic Gln and an arginine finger in *trans*. Deciphering the underlying principles that unify seemingly unrelated mechanisms is central to understanding how diverse mechanisms evolve. Here, we recognize that steric hindrance between active site residues is a criterion governing the mechanism employed by a given GTPase. The Arf−ArfGAP structure is testimony to this concept of spatial (in)compatibility of active site residues. This understanding allows us to predict an as yet unreported hydrolysis mechanism and clarifies unexplained observations about catalysis by Rab11 and the need for HAS-GTPases to employ a different mechanism. This understanding would be valuable for experiments in which abolishing GTP hydrolysis or generating constitutively active forms of a GTPase is important.

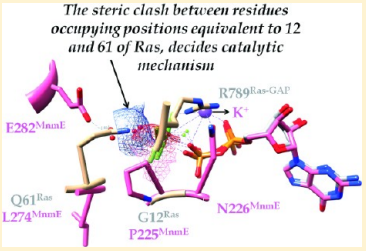

GTP binding proteins or GTPases hydrolyze GTP as a means of regulating a gamut of important cellular processes. The catalytic machinery for GTP hydrolysis lies within a universally conserved G-domain, ~20−25 kDa in size.[1] Residues required for nucleotide binding and hydrolysis are provided by P-loop, switch I, and switch II, which are regions typically present in the G-domain. The GTP hydrolysis reaction has been studied well in classical GTPases such as Ras. In these, the hydrolysis reaction is intrinsically weak and is accelerated by orders of magnitude because of the interaction with GTPase activating proteins (GAPs).[2−7] Hence, efficient GTP hydrolysis by these requires catalytic residues supplied in *cis* by the G-domain and in *trans* by the GAPs. In the case of several Ras superfamily GTPases and also the G-α subunits of heterotrimeric G-proteins, a highly conserved glutamine from the DxxGQ motif present in the switch II region is crucial for catalysis.[8−11] Hereafter, we refer to this Gln as Gln^{cat} when it participates in catalysis (or as Gln^{SwII} when it does not). On one hand, in the aforementioned GTPases, Gln^{cat} is known to activate a catalytic water molecule, which then acts as a nucleophile to attack the γ-phosphate of GTP, which results in its hydrolysis. On the other hand, because of the low pK_a of Gln^{cat}, it was also argued to be ineffective in directly deprotonating the catalytic water.[12] Irrespective of its precise role, the importance of Gln^{cat} for catalysis is well established. However, as this debate is unresolved, in this study we shall assume that Gln^{cat} is known to activate a catalytic water molecule. The developing negative charge on the transition state is neutralized by a positively charged Arg (arginine finger, hereafter termed Arg^{GAP}) supplied in *trans* by the GAP molecule. Given the cardinal role of Gln^{cat} in GTP hydrolysis, substituting it with a hydrophobic residue arrests the protein in the GTP-bound form and renders it constitutively active.[8] Hence, it is not surprising that Gln^{cat} mutations in Ras are oncogenic.[13] However, there exists a subset of GTPases termed HAS-GTPases that naturally possess a hydrophobic residue in lieu of Gln^{cat} and yet efficiently hydrolyze GTP.[14] On the basis of an analysis of HAS-GTPases, Mishra et al.[14] proposed that a catalytic residue that satisfies a role similar to that of Gln^{cat} could arise in *cis* from regions other than switch II or in *trans* from an interacting protein. In tune with this, the transition state structure of MnmE, a HAS-GTPase that contains a Leu in place of Gln^{SwII}, reveals that a highly conserved glutamate (Glu-282) from helix α2 acts as the catalytic residue. Unlike the case in other well-studied GTPases such as Ras, in which Gln^{cat} activates a catalytic water, here Glu-282 facilitates catalysis via a secondary water molecule that in turn activates the identical catalytic water.[15]

In contrast to Ras, MnmE and several other GTPases employ a K^+ ion in lieu of Arg^{GAP} to stabilize the developing negative charge on the transition state. Recently, Ash et al. classified such cation-dependent GTPases into two groups. Group 1 comprises MnmE, Der, YqeH, FeoB, etc., that exhibit enhanced GTPase activity in the presence of K^+ or any other cation with a similar ionic radius. Group 2 on the other hand includes human dynamin and a dynamin-related protein, AtDRP1A, in which GTPase activity is accelerated either by Na^+ or by K^+. Both groups share certain structural features that are responsible for

Received: October 16, 2012
Revised: January 5, 2013
Published: January 7, 2013

   dx.doi.org/10.1021/bi3014054 | *Biochemistry* 2013, 52, 1122−1130

accommodating the cation in the active site; while Ash et al. suggested that GTPases that share such a signature would use a cation-mediated mechanism, we argued in contradiction and showed that these features alone are insufficient to generalize the prevalence of such a mechanism.[16,17] Therefore, understanding diverse hydrolysis mechanisms and their determinants becomes important.

While Gln^{cat} (in classical GTPases) and Glu-282 (in MnmE) are catalytic residues supplied in *cis*, Mishra et al.[14] suggested the possibility of the participation of a catalytic residue in *trans*. Such a mechanism was later found to be employed by Rab33 and Rap1.[18,19] In Rab33, Gln^{SwII} is conserved just like it is in Ras, i.e., DxxGQ. However, it does not participate in catalysis, and instead the GAP, apart from supplying Arg^{GAP}, also supplies Gln^{cat}, but in *trans* to activate the catalytic water; this was termed the "dual-finger mechanism".[18] Rap1 possesses a Thr in place of Gln^{SwII} (DxxGT), which does not participate in catalysis. Instead, an Asn supplied in *trans* by Rap1GAP activates the catalytic water, and Tyr supplied in *cis* by Rap1 plays a role akin to that of Arg^{GAP}.[19,20]

It is now evident from a number of transition state structures of classical GTPases such as Ras that apart from the intrinsic catalytic residue, i.e., the Gln^{cat}, an equally important element for catalysis is the residue supplied by GAP, typically the Arg^{GAP}. Variations to Arg^{GAP} are seen in the form of a Tyr^{GAP} in Ran and Rap1 systems and a monovalent potassium or sodium ion in cation-dependent GTPases.[11,15,21] These residues serve two purposes; they first neutralize the developing negative charge and hence stabilize the transition state, and they second orient the catalytic residue (e.g., Gln^{cat}) to facilitate activation of the nucleophilic water. Except for cation-dependent GTPases, wherein a K^+ or Na^+ ion acts as a GTPase activating element (GAE) to stabilize the transition state,[15] the activating factors for most of the GTPases characterized so far are proteins or RNA. In essence, like the catalytic residue, the activating factor (GAP/GAE), too, exhibits variations. Therefore, it appears that though GTP hydrolysis by GTPases is a common theme for cellular regulation, it is achieved differently by different GTPases. Hence, the factors responsible for eliciting such remarkable variations need to be understood. Here, we have conducted a rigorous analysis of the available transition state structures of GTPases and their primary sequences. This allows us to unify the seemingly different variations in catalytic mechanisms to spatial (in)compatibility between two important active site residues in the P-loop and switch II. The Arf–ArfGAP structure verifies this thinking. This work also explains why HAS-GTPases need to utilize a distinct hydrolysis mechanism as opposed to the classical mechanism seen in Ras-like GTPases.

MATERIALS AND METHODS

Sequence Analysis. Sequences corresponding to Ras superfamily GTPases were obtained from the SMART database.[22] Similarly, sequences of HAS-GTPases and translational GTPases were obtained from INTERPRO and UNIPROT databases.[23,24] Redundancy within the sequences was removed by employing a 90% cutoff using CD-HIT.[25] Following this, multiple-sequence alignment was performed using MUSCLE.[26] Custom-written python scripts using the biopython modules[27,28] were employed to calculate the relative frequency of residues at positions 12 and 61. Conserved residues are depicted as sequence logos using the stand-alone WebLogo program.[29] Ras proteins in cluster I include the closely related Rap1, Di-Ras2, Ral, Rhes, Rsr1, and Rheb. Similarly, Rho in cluster I and Rab in cluster III include all closely related members.

Structural Analysis. Structures of Ras in the ground state [Protein Data Bank (PDB) entry 5p21] and transition state (PDB entry 1wq1), Rab33 in the transition state (PDB entry 2g77), MnmE in the transition state (PDB entry 2gj8), Rho in the transition state (PDB entry 1tx4), Ran in the transition state (PDB entry 1k5g), dynamin in the transition state (PDB entry 2x2e), hGBP1 in the transition state (PDB entry 2b92), AtDRP1A in the transition state (PDB entry 3t34), Arf in the transition state (PDB entry 3lvq), FeoB in the transition state (PDB entry 3ss8), Rab11 (PDB entry 2f9l), Sar1 (PDB entry 1m2o), Rap1 (PDB entry 3brw), IF2 (PDB entry 1g7t), and EF-Tu (PDB entries 1eft and 1ha3) in their GTP- and GDP-bound forms were obtained.[30] Structures were visually inspected, analyzed, and rendered for figures using chimera.[31] Substrate-based structural superpositions[32] were performed using custom-written python scripts based on biopython modules.[27,28]

RESULTS AND DISCUSSION

Clustering GTPases Based on the Coevolution of Active Site Residues. The transition state structure of prototypical GTPase Ras in complex with p120GAP (RasGAP) elucidated the structural basis for GTP hydrolysis and its loss in oncogenic mutants.[8] This structure showed that a hydrophobic substitution in place of Gln-61 (DxxGQ of switch II) and/or non-glycyl substitution of Gly-12 (GxGxxGKS/T of the P-loop) would prevent GTP hydrolysis. Given the role of Gln-61 in abstracting a proton from the catalytic water, the basis for the loss of activity due to its hydrophobic substitution is apparent. However, with respect to non-glycyl substitution at position 12, for the first time it became evident from the structure that the presence of a side chain, even that of an Ala, would sterically clash with the NH_2 group of Gln-61 and the main chain carbonyl of Arg^{GAP}.[8] Therefore, this leads to the loss of both intrinsic and GAP-stimulated GTP hydrolysis. On the basis of this finding, we reasoned that a non-glycyl residue at position 12 and a Gln-like residue at position 61 might not coexist. We further inquired if a coevolution between these sites could operate to preserve the biochemical function, i.e., GTP hydrolysis, and whether this could act as a selection pressure as GTPases evolved. We therefore began a simple analysis of several GTPases (see Materials and Methods) to estimate the frequency of non-glycyl residues at position 12 and the occurrence of hydrophobic residues at position 61. In the proteins we analyzed, evidently the residue numbers equivalent to positions 12 and 61 of Ras are different. However, for the sake of clarity, we have continued referring to these positions as 12 and 61 in all GTPases. The analysis of the nature of residues present at positions 12 and 61 revealed a clear clustering of these GTPases into three distinct groups (Figure 1). Cluster I is composed of GTPases that have predominately Gly at position 12 and Gln at position 61. Cluster II consists of GTPases with a non-glycyl residue at position 12 and a hydrophobic residue at position 61. However, cluster III lies between clusters I and II, its members having a non-glycyl residue at position 12 but a Gln (or His) at position 61. Although simplistic in nature, an analysis of residues at positions 12 and 61 seems to clearly categorize GTPases into these three distinct classes. This prompted a detailed examination of the structure–function relationships for the GTPases in each of these clusters, to

dx.doi.org/10.1021/bi3014054 | *Biochemistry* 2013, 52, 1122–1130

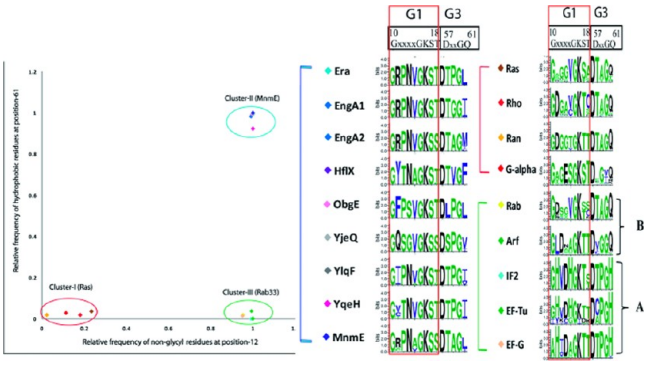

Figure 1. Clustering GTPases based on the nature of the residues at positions 12 and 61. The scatter plot shows the relative frequency of hydrophobic residues at position 61 vs non-glycyl residues at position 12. Values on the *X* and *Y* axes indicate the relative frequencies (for details, see Materials and Methods). Clusters I–III are indicated. The families of proteins contained in each of these clusters are displayed at the right, along with the corresponding G1 (red box) and G3 motifs that harbor positions 12 and 61, respectively; these are depicted as sequence logos (see Materials and Methods). The height of the logo represents the extent of conservation of a given residue within a family. The residues in G1 (red box) and G3 motifs are shown above the logos, where the residue numbers (superscript) correspond to those in Ras. For generating sequence logos of certain families of GTPases like Ras, Rho, and Rab, sequences of closely related subfamilies were also included (see Materials and Methods). Cluster III is further subdivided into groups A and B (see the Supporting Information).

evaluate the nature of interactions between the side chains of residues 12 and 61.

Spatial Constraints between Residues Occupying Positions 12 and 61. To understand the role of residues at positions 12 and 61 in GTP hydrolysis, the three-dimensional (3D) structures in the transition state are required. Hence, only those GTPases for which transition state structures are available were chosen as representatives. The transition state structures of Ras, the G-α subunit of heterotrimeric G-proteins, and Rho GTPases, which are members of cluster I, show that the mechanism of GTP hydrolysis in these proteins is conserved. Hence, for this study, Ras was chosen to represent the cluster I GTPases (Figure 1), which possess Gly and Gln at positions 12 and 61, respectively. In these, the presence of Gly at position 12 prevents a steric clash with Gln at position 61. On the other hand, MnmE, which represents cluster II (Figure 1), has a Pro at position 12 and lacks a Gln or a hydrophilic residue at position 61. A substrate-based structural superposition of the Ras–RasGAP complex and MnmE shows that position 12 in Ras is occupied by a Gly so that Gln-61 could approach the active site, while in MnmE, a hydrophobic Leu at position 61 is retracted from the active site and thus prevents a steric clash with Pro at position 12 (Figure 2a). In hGBP1, too, a Tyr residue is found at position 12, and similarly, a Leu at position 61 is retracted from the active site to prevent a steric clash with the Tyr (see Figure 4).

Rab33, which represents cluster III (Figure 1), presents remarkable variation. Members of this cluster have a non-glycine residue at position 12 and a hydrophilic residue at position 61: Rab33 has a glutamine (Gln-92) at position 61. A superposition of Rab33–TBC-GAP and Ras–RasGAP complexes, shown in Figure 2b, depicts that Gln^{SwII} (Q92 in Figure 2b) surprisingly does not participate in catalysis and is instead oriented away from the nucleotide. In contrast, a Gln^{cat} (Q378 in Figure 2b) provided in *trans* by the TBC-GAP domain takes over the catalytic role akin to that of Gln^{cat} of Ras (Q61 in Figure 2b); the terminal atoms of these Gln^{cat} residues in the TBC-GAP domain and Ras occupy identical three-dimensional positions to activate a catalytic water. The reason for this unusual phenomenon termed the dual-finger mechanism,[18] wherein both Gln^{cat} and Arg^{GAP} are supplied in *trans* by the TBC-GAP domain, was not comprehendible. An inspection of the structural superposition in Figure 2b allows us to attribute the nonutilization of the Gln^{SwII} in Rab33 to the presence of a Ser (S42 in Figure 2b), and not a Gly at position 12. Another consequence is that this Ser, apart from occluding Gln^{SwII}, would also occlude the entry of the Arg^{GAP}, if the direction in which Arg^{GAP} is inserted into the active site was the same as in cluster I GTPases (Figure 2b). Interestingly, the in *trans* Arg^{GAP} from the TBC-GAP domain is inserted in a manner that prevents the steric clash with Ser at position 12 (Figure 2b). Therefore, the deployment of the dual fingers from the TBC-GAP domain appears to be a means of overcoming the constraint posed by a non-glycyl residue at position 12 in Rab33. On the basis of this, we speculate that a similar situation would also prevail in the Rab11 subfamily GTPases involved in recycling endosomes. In these, Gln-70 (equivalent to Gln-61 of Ras) was anticipated to play a catalytic role. However, as its mutation to a Leu (Q70L) did not affect GTP hydrolysis,[33,34] it was implicated to be noncatalytic. This observation has thus far not been explained. A similar analysis of Rab11 revealed that it possesses a highly conserved Ser at position 12 (Ser-20 in Rab11). Therefore, it might be that spatial constraints, similar to that in Rab33, operate between residues at position 12 (Ser-20) and position 61 (Gln-70) and occlude it from activating the catalytic water. Perhaps Gln-70 is the noncatalytic Gln^{SwII}, equivalent to Gln-92 of Rab33. This may explain why the Q70L mutation is inconsequential to GTP hydrolysis in Rab11.[33] This implies that Rab11 does not utilize Q70 but an alternative catalytic residue to activate the water molecule; this needs to be identified. Further structural studies would be necessary to reveal the mechanism by which Rab11 prevents the steric clash between Ser-20 and Gln-70, and whether a TBC-GAP, like for Rab33, provides the catalytic glutamine *in trans*.

Apart from Rab33, GTPases involved in translation such as IF2, EF-Tu, and EF-G are also members of cluster III. They possess a highly conserved His at position 61 and a Val or an Ile at position 12. The importance of His at position 61 for GTP hydrolysis is underscored by the available biochemical and computational studies on EF-Tu.[35−37] However, the absence of transition state (TS) crystal structure(s) for these GTPases precludes a comprehensive understanding of how this His may participate in catalysis despite the presence of a non-glycyl residue at position 12. We therefore resorted to the analysis of the available crystal structures, i.e., EF-Tu bound to GTP and EF-Tu bound to GDP and aurodox, although these were determined in the ground state (GS). In these structures, His at position 61 adopts two distinct conformations, both of which surprisingly prevent a steric clash with the side chains at position 12 (Figure 3). In Ras, Gln^{cat} adopts catalytically active and inactive conformations in the transition state (TS) and ground state (GS) structures, respectively (note the position of Q61 in Figure 3a,b). The two conformations of His in EF-Tu appear to resemble these. An inactive conformation is seen in GTP-bound EF-Tu (H85 in Figure 3a), where it appears to be incompetent to activate the catalytic water. On the other hand, in the structure of EF-Tu in complex with GDP and aurodox

dx.doi.org/10.1021/bi3014054 | *Biochemistry* 2013, 52, 1122−1130

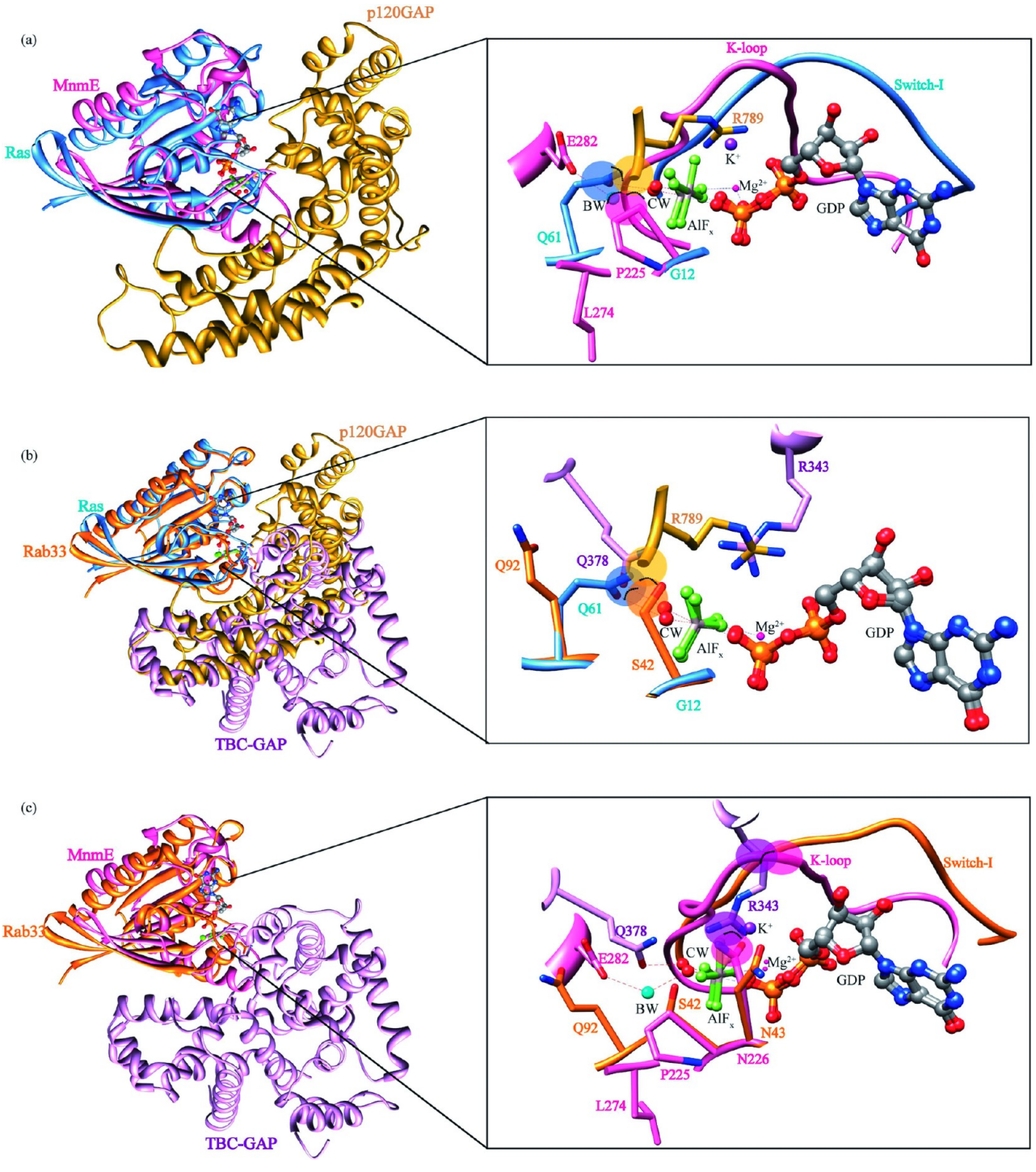

Figure 2. Spatial constraints between active site residues in the three classes of GTPases. Substrate-directed superposition of Ras (cluster I), MnmE (cluster II), and Rab33 (cluster III) transition state structures. Ras is displayed as blue ribbons; Rab33 is colored orange, MnmE pink, p120GAP (RasGAP) gold, and the TBC-GAP domain light violet. An overlay of the active sites is shown in the insets. The amino acid residues are shown as sticks with O atoms colored red and N atoms blue. GDP and AlF_x are depicted as balls and sticks (C, dark gray; O, red; P, orange; F, light green; Al, light gray). Mg^{2+} and K^+ ions are represented as dark pink and violet balls, respectively. The catalytic water (CW) is displayed as a red ball, while the bridging water (BW) is shown as a blue ball. The van der Waals surface is depicted as a sphere encircling the corresponding atoms, and a steric clash is indicated by a dotted arc. Comparisons of active sites between (a) Ras and MnmE, (b) Ras and Rab33, and (c) Rab33 and MnmE illustrate the spatial constraints between positions 12 and 61.

(an antibiotic),[38] a catalytically active conformation of His is seen (H85 in Figure 3b). This conformation appears to be competent to activate a water molecule. Recent molecular dynamics simulation studies, the cryo-EM structure of the EF-Tu−ribosome complex, and biochemical studies of the EF-G−ribosome complex suggest the involvement of rRNA in repositioning His toward the catalytically active conformation for GTP hydrolysis.[37,39,40] The crystal structure of EF-Tu and aminoacyl-tRNA bound to the ribosome depicts that the base A2662 of the sarcin−ricin loop of the 23S rRNA is required to

dx.doi.org/10.1021/bi3014054 | *Biochemistry* 2013, 52, 1122−1130

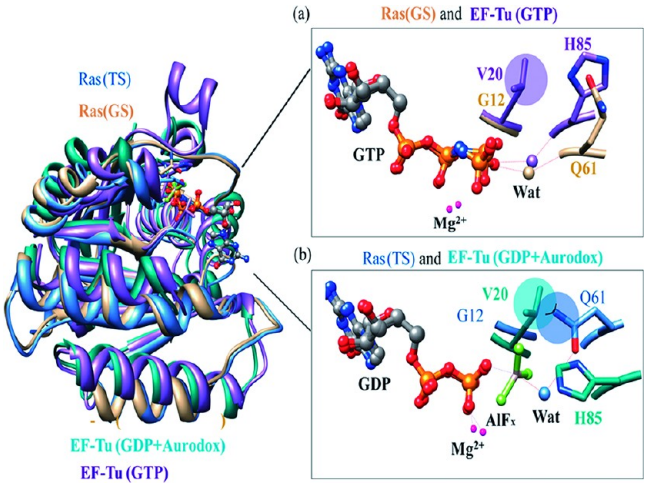

Figure 3. Comparison of spatial constraints in the active sites of Ras and EF-Tu. Substrate-directed superposition of Ras bound to GTP [Ras(GS)], Ras bound to GDP-AlF$_x$ [Ras(TS)], EF-Tu bound to GTP, and EF-Tu bound to GDP and aurodox is shown in the left panel. Ras(GTP) is shown as a brown ribbon, and Ras(TS) is colored blue, EF-Tu bound to GTP violet, and EF-Tu bound to GDP and aurodox dark green. The active sites in (a) Ras(GS) bound to GTP and EF-Tu bound to GTP are compared with those in (b) Ras(TS), i.e., bound to GDP-AlF$_x$ and EF-Tu bound to GDP and aurodox. The amino acid residues are shown as sticks; nucleotides GTP and GDP are shown as balls and sticks, and Mg^{2+} and the catalytic water (wat) are shown as spheres with O atoms colored red and N atoms blue. GDP, GTP, and AlF$_x$ are depicted as balls and sticks (C, dark gray; O, red; P, orange; F, light green; Al, light gray). Mg^{2+} is represented as a dark pink ball. The catalytic water (wat) is colored in concordance with the colors used for the proteins. The van der Waals sphere for the side chains at positions 12 and 61 is indicated. It can be seen that the side chain of H85 adopts two distinct conformations in panels a and b coinciding with the ground state and transition state conformations of Q61, respectively. A steric clash between the side chain atoms of V20 and Q61 (in TS), but not with H85, may be noticed in panel b.

orient the histidine of EF-Tu in a catalytically competent conformation to activate the nucleophilic water.[41] However, a recent work by Zhou et al.[42] contradicts this view, and the absence of a transition state structure prohibits verification of either claim. Incidentally, similar active conformations of His at position 61 are also observed in the ground state structures of IF2[43] and Sar1,[44] which are members of cluster III as well.

Spatial Constraints on the Usage of GAP Machinery. The participation of residues from the GAP is also needed for efficient GTP hydrolysis. Therefore, apart from analyzing spatial constraints between residues at positions 12 and 61, we found it becomes necessary to examine constraints arising due to the residue provided by the GAP. Besides the variations noted in the usage of a catalytic residue at position 61, catalytic residues provided by GAPs also vary in the type of residues and the manner in which they are employed. In Ras and Rho of cluster I, it is an Arg^{GAP} that is inserted from the switch I side (R789 in Figure 2a). An exception is seen in the HAS-GTPase MnmE (of cluster II) where a monovalent K^+ ion stabilizes the transition state and occupies a position identical to the terminal atoms of Arg^{GAP} of cluster I[15] (Figure 2a). To understand the spatial constraints posed by the GAP residue or K^+ ion, we first compared the transition state structures of MnmE and Ras. Three features seem to occlude the entry of a GAP residue into the active site of MnmE. The first is an Asn-226 in the P-loop, equivalent to Gly-13 in Ras that coordinates the K^+ ion (Figure 2c). The second is a part of switch I, termed the K-loop that coordinates the K^+ ion (Figure 2c). The third is a Pro at position 12, whose side chain would result in a steric clash with the main chain carbonyl of Arg^{GAP} (R789 in Figure 2a). This clash is avoided in the Rab33 system, wherein an in *trans* Arg^{GAP} is supplied from a different direction as discussed above (note R789 vs R343 in Figure 2b). Nonetheless, and remarkably, the relative 3D positions occupied by the guanidinium groups of the two Arg^{GAP} residues, R789 and R343, to stabilize the transition states in Ras and Rab33 remain unaltered. In the case of MnmE, however, an in *trans* Arg^{GAP} as in Rab33 may not to be utilized, as it would continue to clash with the K-loop (Figure 2c). Hence, in MnmE, it appears that the spatial constraints imposed by positions 12 and 13 and the specific conformation adopted by the K-loop would occlude the entry of an Arg^{GAP}-like residue and, therefore, the need for a K^+ ion to stabilize the transition state.

Like MnmE, several cation-dependent GTPases share structural features responsible for accommodating a K^+ ion in the active site.[16] Recently, dynamins, important mediators of endocytosis, were reported to utilize a mechanism similar to that of MnmE, except that they use a Na^+ in place of a K^+ ion.[21] While the catalytic residue in this case is different and is also supplied from a different direction, here too, the catalytic water is activated via bridging water like in MnmE. Interestingly, dynamins and MmmE belong to the family of HAS-GTPases that do not possess a Gln at position 61. Several HAS-GTPases conserve a non-glycine residue at position 12, and some also possess an Asn at position 13. Therefore, it is evident that the non-glycyl side chain of position 12 would cause steric hindrance and occlude a Gln, if it were to be present at position 61 in HAS-GTPases (Table S1 of the Supporting Information). Hence, it is evident that HAS-GTPases need to employ a mechanism that does not utilize an in *cis* Gln from position 61. However, not all HAS-GTPases contain a K-loop to stably bind a cation. We suggest that such GTPases may utilize a novel mechanism (discussed below).

hGBP1 is an interferon-γ-induced GTPase that shares a high degree of structural similarity with dynamins. Lacking a Gln at position 61, it too was classified as a HAS-GTPases. Interestingly, hGBP1 uses a distinct mechanism than that of MnmE and dynamins and the classical GTPases.[45] A comparison of the transition state structures of Ras and hGBP1 reveals that similar spatial constraints due to a Tyr at position 12 and a Leu at position 61 are operative in hGBP1, too (Figure 4). It is evident that the entry of an Arg^{GAP} into the active site would be occluded by the steric clash with Tyr (at position 12). Two consequences of this occlusion appear to be (1) a Leu at position 61 retracts from the active site and instead a Ser at position 73 from switch I activates the catalytic water and (2) it employs an Arg^{GAP}, but in *cis*. The employment of the latter appears reasonable, as hGBP1 possesses the characteristic K-loop of the cation-dependent GTPases, which occludes an in *trans* entry of Arg^{GAP} from the alternative direction, as in the Rab33−TBC-GAP system. Further in hGBP1, in place of the conserved P-loop Asn (that coordinates K^+ in cation-dependent GTPases), an Arg^{GAP} directly stabilizes the transition state (Figure 4). In summary, here, a Ser from switch I directly activates the catalytic water, while an Arg^{GAP} from the P-loop is utilized to stabilize the transition state.

On the basis of a simplistic extrapolation to the catalytic mechanisms discussed thus far, it is possible to envisage an as yet unexploited catalytic mechanism. It would involve the usage

dx.doi.org/10.1021/bi3014054 | *Biochemistry* 2013, 52, 1122−1130

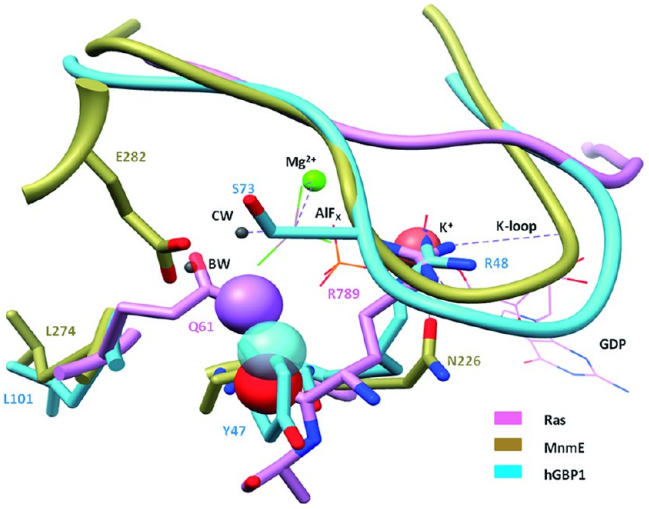

Figure 4. Spatial constraints on the usage of GAP machinery in hGBP1. A substrate-based superposition of the transition state structures of Ras (cluster I), MnmE (cluster II), and hGBP1 (cluster II) is shown. Ras and p120GAP are displayed as a light violet ribbon, and hGBP1 is colored blue and MnmE gold. An overlay of the active sites is shown in the inset. GDP and AlF_x are depicted as wires (O, red; N, blue; F, light green; Al, light gray). Mg^{2+} and K^+ ions are represented as green and pink spheres, respectively. The catalytic water (CW) as well as the bridging water (BW) is displayed as a gray sphere. The van der Waals surface is depicted as a sphere encircling the corresponding atoms, and a steric clash is indicated by an overlap. A comparison of the transition state structures of Ras, hGBP1, and MnmE reveals that spatial constraints imposed on the entry of an Arg^{GAP}, due to a Tyr (Y47) at position 12 and a Leu (L101) at position 61, is relieved by providing an in *cis* Arg^{GAP} (R48) from the P-loop to stabilize the transition state. Also, a Ser (S73) from switch I directly activates the catalytic water.

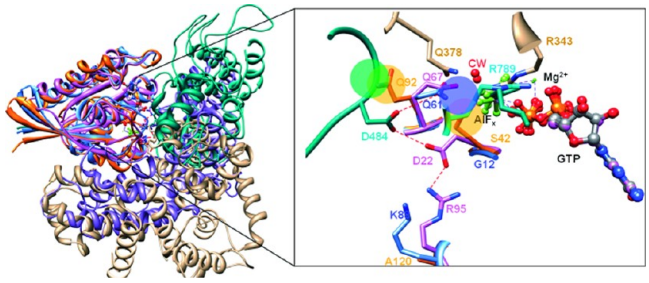

Figure 5. Analysis of the Arf–ArfGAP transition state structure. Substrate-directed superposition of the transition state structures of Ras (cluster I), Rab33 (cluster II), and Arf (cluster II) is shown. Ras is displayed as blue ribbons, and Rab33 is colored orange, Arf pink, p120GAP light cyan, the TBC-GAP domain light brown, and ArfGAP dark cyan. An overlay of the active sites is shown in the inset. The amino acid residues are shown as sticks with O atoms colored red and N atoms blue. GDP and AlF_x are depicted as balls and sticks (C, dark gray; O, red; P, orange; F, light green; Al, light gray). The Mg^{2+} ion is represented by a green ball and the catalytic water (CW) by a red ball. The van der Waals surface is depicted as a sphere encircling the corresponding atoms, and a steric clash is indicated by the overlap of the spheres. Comparison of active sites among Ras, Rab33, and Arf indicates that the participation of $Q67^{Arf}$ in catalysis is facilitated by $D22^{Arf}$–$D484^{ArfGAP}$ and $D22^{Arf}$–$R95^{Arf}$ stabilizing interactions as well as the steric constraints imposed by the loop (dark cyan) of ArfGAP, which also provides D484.

of Arg^{GAP} as in cluster I and III GTPases and a bridging water-mediated activation of catalytic water as in MnmE and dynamins. Given this, it is possible to speculate that the aforementioned mechanism may be operative for those HAS-GTPases lacking a K-loop-like feature. Such GTPases may utilize a hybrid of mechanisms noted for MnmE and Rab33–TBC-GAP systems. We speculate that in such GTPases, the conserved Asn at position 13 would occlude usage of Arg^{GAP} if it were used like in the Ras–RasGAP system, and because the absence of a K-loop precludes the stabilization of K^+ or Na^+ ion, it would still allow the entry of Arg^{GAP} from an alternative direction like in the Rab33 system. It will be interesting to see whether future studies confirm the presence of such a mechanism.

The Arf–ArfGAP Crystal Structure Substantiates the Theory of Spatial (In)compatibility. The importance of spatial compatibility between active site residues, deciphered in this work, is further reinforced by the Arf–ArfGAP transition state crystal structure.[46] Arf belongs to GTPase cluster III with an Asp at position 12 and a Gln at position 61. On the basis of the current analysis, one would have anticipated that Arf would use the dual-finger mechanism like Rab33; i.e., ArfGAP would provide a *trans*-Gln. Counterintuitively, Arf uses the *cis*-Gln effectively for catalysis. The importance of spatial compatibility is evident from this structure. Here, the presence of Asp (D22) at position 12 would deter the participation of Gln from position 61, and hence, a retracted conformation of *cis*-Gln (as with Rab33) is anticipated. However, surprisingly, the *cis*-Gln ($Q67^{Arf}$) of Arf does participate in catalysis. This is explained by a substrate-based superimposition of Ras–RasGAP, Rab33–TBC-GAP, and Arf–ArfGAP transition state structures. The superposition reveals that $Q67^{Arf}$, unlike $Q92^{Rab33}$, cannot retract from the active site because a loop from ArfGAP would have been sterically hindered with $Q67^{Arf}$ if it had adopted a retracted conformation (Figure 5). While ArfGAP restricts a retracted conformation of $Q67^{Arf}$, conversely, the presence of $D22^{Arf}$ at position 12 would also disallow a catalytically competent conformation of $Q67^{Arf}$. This would lead to Arf being catalytically inactive, unless one of these constraints is relieved. Interestingly, two distinct interactions stabilize $D22^{Arf}$ in an alternative conformation that relieves the steric clash with $Q67^{Arf}$: one of these is provided by the same loop of ArfGAP that impedes the retracted conformation of $Q67^{Arf}$, and the other is provided by a conserved residue, $R95^{Arf}$ (see $D22^{Arf}$–$D484^{ArfGAP}$ and $D22^{Arf}$–$R95^{Arf}$ in Figure 5). These interactions allow the in *cis* Gln $Q67^{Arf}$ to play a catalytic role. This structure not only verifies the importance of spatial compatibility of active site residues but also raises interesting questions. In light of the retraction of $D22^{Arf}$, why is this possibility not seen for the Rab33 system? First, Rab33 possesses A120 in place of $R95^{Arf}$ (Figure 5). Second, unlike ArfGAP, the TBC-GAP domain does not impede the retraction of $Q92^{Rab33}$. Hence, it appears that steric constraints and stabilizing interactions provided by the GAP direct the participation of $Q67^{Arf}$ in catalysis. This is further evidence of the structural plasticity in the GTPase systems.

This analysis also prompted us to inquire how the diverse GTP hydrolysis mechanisms may have evolved. Given the importance of the spatial compatibility between positions 12 and 61 in the diverse mechanisms, we examined the possible evolution of these by following mutational changes between positions 12 and 61. Interestingly, cluster III GTPases like IF2, EF-Tu, and EF-G (Figure 1) follow a distinct mechanism as

dx.doi.org/10.1021/bi3014054 | *Biochemistry* 2013, 52, 1122–1130

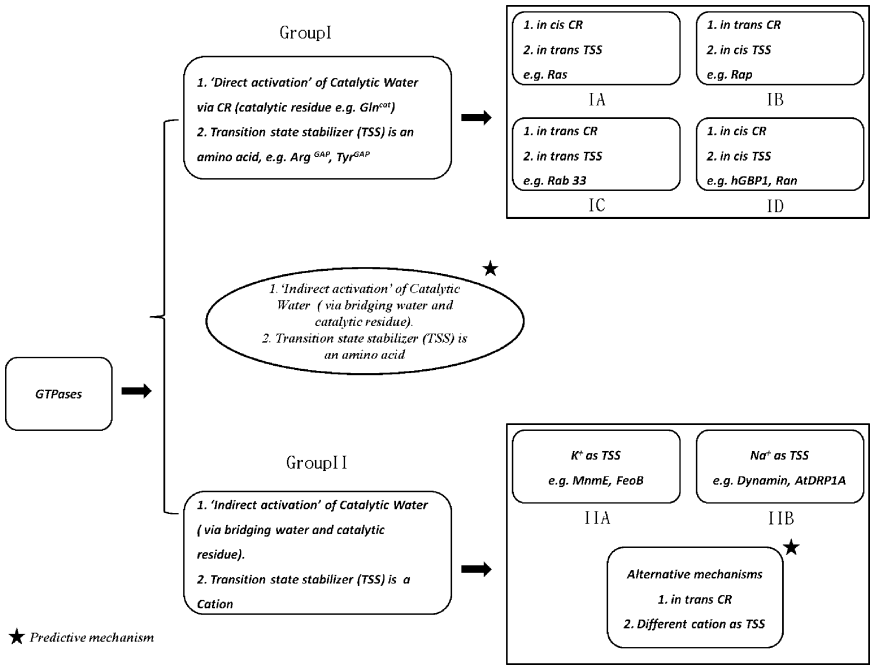

Figure 6. Clustering GTP hydrolysis mechanisms. Our analysis reveals that GTP hydrolysis mechanisms (and not GTPases) could also be distinguished, as shown here. The basis for this division into group I and group II is dependent on whether the catalytic water is activated directly or indirectly. Whenever the activation is direct, an amino acid appears to participate in stabilizing the transition state. In contrast, a cation seems to satisfy this role, when the activation is mediated indirectly via a bridge water. Further subdivision of these groups is based on either the nature of the cations or whether these factors (CR and TSS) are supplied in *cis* or in *trans*. Mechanisms that may in principle operate in GTPases (predictive mechanisms) are also shown here.

they possess a catalytic histidine, but not a glutamine at position 61; these have a Val at position 12. For reasons elaborated in the Supporting Information, these translational GTPases were considered to be closest to the last universal common ancestor (LUCA).[47] Considering Val and His of IF2 to be the residues occupying positions 12 and 61, respectively, of the ancient GTP hydrolysis machinery, how could the current variations in catalytic mechanisms evolve? A speculative model attempting to answer this question is also provided in the Supporting Information.

Apart from the classification suggested in Figure 1, the diverse mechanisms employed by GTPases could be grouped differently. Such a classification would divide GTPases into two major groups based on mechanistic similarities or differences, rather than the nature of residues at positions 12 and 61 alone. In this scheme shown in Figure 6, group I would involve a catalytic residue (CR) that activates the catalytic water "directly", and these always employ an amino acid (like Arg^{GAP} or Tyr^{GAP}) to stabilize the transition state [transition state stabilizer (TSS)]. Further subdivision of this group may depend on the in *cis* or in *trans* employment of these factors, as illustrated in Figure 6. What is common to all of these is the direct activation of the nucleophilic water. In contrast, the second major group would reflect the mechanism seen in MnmE, dynamins, etc., in which a catalytic residue is located at a position other than position 61 and "indirectly" activates the catalytic water via a bridging water molecule. These do not seem to employ an Arg^{GAP} but a cation to stabilize the transition state (Figure 6). Interestingly, the new mechanism proposed previously would lie between those of the two major groups, as shown in Figure 6. In fact, it is possible to envisage more variations. For example, in group II, different modes (other than the K-loop) of stabilizing the cation may be realized, or other cations may be utilized to stabilize the transition state, or the catalytic residue may be supplied in *trans*. Will GTPases utilize all of these possibilities? Future studies will answer this question.

This work is immediately relevant to the experimental biologist because of the following. For several cell biology and localization studies, "constitutively active forms" (i.e., arrested in a GTP-bound state) of GTPases are achieved by mutating the residue equivalent to Gln61 (of Ras). While addressing the biochemistry, this mutation is anticipated to abolish all GTP hydrolysis. Usually, this residue is identified by aligning the primary sequence of the GTPase in question with that of Ras or other well-studied members. However, this strategy would identify the catalytic Gln (and hence its mutation would yield a constitutively active form) only when the GTPase belongs to group IA, but not when it belongs to group I or II (Figure 6). This was indeed the case with Rab11 GTPases, where the Q70L mutation did not result in the loss of GTP hydrolysis because it utilizes the mechanism of group IC. With emerging variations in GTP hydrolysis mechanisms, it therefore becomes important to inquire about the mechanism likely operative in the GTPase. Our analysis should guide the assessment of this important aspect, such that experiments may be designed appropriately.

■ ASSOCIATED CONTENT

Supporting Information

Translational GTPases and evolution of GTP hydrolysis mechanisms and Tables S1 and S2. This material is available free of charge via the Internet at http://pubs.acs.org.

dx.doi.org/10.1021/bi3014054 | *Biochemistry* 2013, 52, 1122−1130

AUTHOR INFORMATION

Corresponding Author

*Telephone: +91-512-2594024. Fax: +91-512-2594010. E-mail: bprakash@iitk.ac.in.

Present Address

[†]Department of Biotechnology, Indian Institute of Technology, Guwahati 781039, India.

Funding

This work was supported by grants from the Department of Biotechnology, India [Grant BT/HRD/34/01/2009(V)], the Department of Science and Technology, India (Grant SR/SO/BB-43/2009), and the Indian Council of Medical Research (Grant 5/8/9/86/2008-ECD-1). B.A. acknowledges AICTE for the National Doctoral Fellowship. S.M. acknowledges CSIR for a fellowship.

Notes

The authors declare no competing financial interest.

ACKNOWLEDGMENTS

We acknowledge all members of the Prakash laboratory for help at various stages of the work.

ABBREVIATIONS

GAP, GTPase activating protein; GAE, GTPase activating element; HAS-GTPase, hydrophobic amino acid-substituted GTPase; LUCA, last universal common ancestor; TBC, Tre-2, Bub2, Cdc16; GS, ground state; TS, transition state; CR, catalytic residue; TSS, transition state stabilizer.

REFERENCES

(1) Vetter, I. R., and Wittinghofer, A. (2001) The guanine nucleotide-binding switch in three dimensions. *Science 294*, 1299−1304.

(2) Geyer, M., and Wittinghofer, A. (1997) GEFs, GAPs, GDIs and effectors: Taking a closer (3D) look at the regulation of Ras-related GTP-binding proteins. *Curr. Opin. Struct. Biol. 7*, 786−792.

(3) Reynaud, E. G., Andrade, M. A., Bonneau, F., Ly, T. B., Knop, M., Scheffzek, K., and Pepperkok, R. (2005) Human Lsg1 defines a family of essential GTPases that correlates with the evolution of compartmentalization. *BMC Biol. 3*, 21.

(4) Sprang, S. R., Chen, Z., and Du, X. (2007) Structural basis of effector regulation and signal termination in heterotrimeric Gα proteins. *Adv. Protein Chem. 74*, 1−65.

(5) Bos, J. L., Rehmann, H., and Wittinghofer, A. (2007) GEFs and GAPs: Critical elements in the control of small G proteins. *Cell 129*, 865−877.

(6) Tcherkezian, J., and Lamarche-Vane, N. (2007) Current knowledge of the large RhoGAP family of proteins. *Biol. Cell 99*, 67−86.

(7) Inoue, H., and Randazzo, P. A. (2007) Arf GAPs and their interacting proteins. *Traffic 8*, 1465−1475.

(8) Scheffzek, K., Ahmadian, M. R., Kabsch, W., Wiesmüller, L., Lautwein, A., Schmitz, F., and Wittinghofer, A. (1997) The Ras-RasGAP complex: Structural basis for GTPase activation and its loss in oncogenic Ras mutants. *Science 277*, 333−338.

(9) Sondek, J., Lambright, D. G., Noel, J. P., Hamm, H. E., and Sigler, P. B. (1994) GTPase mechanism of G-proteins from the 1.7-Å crystal structure of transducin α-GDP-AIF-4. *Nature 372*, 276−279.

(10) Rittinger, K., Walker, P. A., Eccleston, J. F., Smerdon, S. J., and Gamblin, S. J. (1997) Structure at 1.65 Å of RhoA and its GTPase-activating protein in complex with a transition-state analogue. *Nature 389*, 758−762.

(11) Seewald, M. J., Korner, C., Wittinghofer, A., and Vetter, I. R. (2002) RanGAP mediates GTP hydrolysis without an arginine finger. *Nature 415*, 662−666.

(12) Schweins, T., Langen, R., and Warshel, A. (1994) Why have mutagenesis studies not located the general base in ras p21. *Nat. Struct. Biol. 1*, 476.

(13) Der, C. J., Finkel, T., and Cooper, G. M. (1986) Biological and biochemical properties of human rasH genes mutated at codon 61. *Cell 44*, 167−176.

(14) Mishra, R., Gara, S. K., Mishra, S., and Prakash, B. (2005) Analysis of GTPases carrying hydrophobic amino acid substitutions in lieu of the catalytic glutamine: Implications for GTP hydrolysis. *Proteins 59*, 332−338.

(15) Scrima, A., and Wittinghofer, A. (2006) Dimerisation-dependent GTPase reaction of MnmE: How potassium acts as GTPase-activating element. *EMBO J. 25*, 2940−2951.

(16) Ash, M. R., Maher, M. J., Guss, J. M., and Jormakka, M. (2012) The cation-dependent G-proteins: In a class of their own. *FEBS Lett. 586*, 2218−2224.

(17) Rafay, A., Majumdar, S., and Prakash, B. (2012) Exploring potassium-dependent GTP hydrolysis in TEES family GTPases. *FEBS Open Bio 2*, 173−177.

(18) Pan, X., Eathiraj, S., Munson, M., and Lambright, D. G. (2006) TBC-domain GAPs for Rab GTPases accelerate GTP hydrolysis by a dual-finger mechanism. *Nature 442*, 303−306.

(19) Daumke, O., Weyand, M., Chakrabarti, P. P., Vetter, I. R., and Wittinghofer, A. (2004) The GTPase-activating protein Rap1GAP uses a catalytic asparagine. *Nature 429*, 197−201.

(20) Scrima, A., Thomas, C., Deaconescu, D., and Wittinghofer, A. (2008) The Rap-RapGAP complex: GTP hydrolysis without catalytic glutamine and arginine residues. *EMBO J. 27*, 1145−1153.

(21) Chappie, J. S., Acharya, S., Leonard, M., Schmid, S. L., and Dyda, F. (2010) G domain dimerization controls dynamin's assembly-stimulated GTPase activity. *Nature 465*, 435−440.

(22) Schultz, J., Milpetz, F., Bork, P., and Ponting, C. (1998) SMART, a simple modular architecture research tool: Identification of signaling domains. *Proc. Natl. Acad. Sci. U.S.A. 95*, 5857−5864.

(23) Apweiler, R., Attwood, T., Bairoch, A., Bateman, A., Birney, E., Biswas, M., Bucher, P., Cerutti, L., Corpet, F., Croning, M., Durbin, R., Falquet, L., Fleischmann, W., Gouzy, J., Hermjakob, H., Hulo, N., Jonassen, I., Kahn, D., Kanapin, A., Karavidopoulou, Y., Lopez, R., Marx, B., Mulder, N., Oinn, T., Pagni, M., Servant, F., Sigrist, C., and Zdobnov, E. (2001) The InterPro database, an integrated documentation resource for protein families, domains and functional sites. *Nucleic Acids Res. 29*, 37−40.

(24) Apweiler, R., Bairoch, A., Wu, C., Barker, W., Boeckmann, B., Ferro, S., Gasteiger, E., Huang, H., Lopez, R., Magrane, M., Martin, M., Natale, D., O'Donovan, C., Redaschi, N., and Yeh, L. (2004) UniProt: The Universal Protein knowledgebase. *Nucleic Acids Res. 32*, D115−D119.

(25) Li, W., and Godzik, A. (2006) Cd-hit: A fast program for clustering and comparing large sets of protein or nucleotide sequences. *Bioinformatics 22*, 1658−1659.

(26) Edgar, R. (2004) MUSCLE: Multiple sequence alignment with high accuracy and high throughput. *Nucleic Acids Res. 32*, 1792−1797.

(27) Cock, P. J., Antao, T., Chang, J. T., Chapman, B. A., Cox, C. J., Dalke, A., Friedberg, I., Hamelryck, T., Kauff, F., Wilczynski, B., and de Hoon, M. J. (2009) Biopython: Freely available python tools for computational molecular biology and bioinformatics. *Bioinformatics 25*, 1422−1423.

(28) Hamelryck, T., and Manderick, B. (2003) PDB file parser and structure class implemented in python. *Bioinformatics 19*, 2308−2310.

(29) Crooks, G., Hon, G., Chandonia, J., and Brenner, S. (2004) WebLogo: A sequence logo generator. *Genome Res. 14*, 1188−1190.

(30) Kabsch, W., Gast, W. H., Schulz, G. E., and Leberman, R. (1977) Low resolution structure of partially trypsin-degraded polypeptide elongation factor, EF-TU, from *Escherichia coli*. *J. Mol. Biol. 117*, 999−1012.

(31) Pettersen, E. F., Goddard, T. D., Huang, C. C., Couch, G. S., Greenblatt, D. M., Meng, E. C., and Ferrin, T. E. (2004) UCSF Chimera: A Visualization System for Exploratory Research and Analysis. *J. Comput. Chem. 25*, 1605−1612.

(32) Kosloff, M., and Selinger, Z. (2003) GTPase catalysis by Ras and other G-proteins: Insights from substrate directed superimposition. *J. Mol. Biol. 331*, 1157−1170.
(33) Pasqualato, S., Senic-Matuglia, F., Renault, L., Goud, B., Salamero, J., and Cherfils, J. (2004) The structural GDP/GTP cycle of Rab11 reveals a novel interface involved in the dynamics of recycling endosomes. *J. Biol. Chem. 279*, 11480−11488.
(34) Scapin, S., Carneiro, F., Alves, A., Medrano, F., Guimarães, B., and Zanchin, N. (2006) The crystal structure of the small GTPase Rab11b reveals critical differences relative to the Rab11a isoform. *J. Struct. Biol. 154*, 260−268.
(35) Daviter, T., Wieden, H., and Rodnina, M. (2003) Essential role of histidine 84 in elongation factor Tu for the chemical step of GTP hydrolysis on the ribosome. *J. Mol. Biol. 332*, 689−699.
(36) Scarano, G., Krab, I., Bocchini, V., and Parmeggiani, A. (1995) Relevance of histidine-84 in the elongation factor Tu GTPase activity and in poly(Phe) synthesis: Its substitution by glutamine and alanine. *FEBS Lett. 365*, 214−218.
(37) Grigorenko, B., Shadrina, M., Topol, I., Collins, J., and Nemukhin, A. (2008) Mechanism of the chemical step for the guanosine triphosphate (GTP) hydrolysis catalyzed by elongation factor Tu. *Biochim. Biophys. Acta 1784*, 1908−1917.
(38) Vogeley, L., Palm, G., Mesters, J., and Hilgenfeld, R. (2001) Conformational change of elongation factor Tu (EF-Tu) induced by antibiotic binding. Crystal structure of the complex between EF-Tu.GDP and aurodox. *J. Biol. Chem. 276*, 17149−17155.
(39) Villa, E., Sengupta, J., Trabuco, L. G., LeBarron, J., Baxter, W. T., Shaikh, T. R., Grassucci, R. A., Nissen, P., Ehrenberg, M., Schulten, K., and Frank, J. (2009) Ribosome-induced changes in elongation factor Tu conformation control GTP hydrolysis. *Proc. Natl. Acad. Sci. U.S.A. 106*, 1063−1068.
(40) Clementi, N., Chirkova, A., Puffer, B., Micura, R., and Polacek, N. (2010) Atomic mutagenesis reveals A2660 of 23S ribosomal RNA as key to EF-G GTPase activation. *Nat. Chem. Biol. 6*, 344−351.
(41) Voorhees, R. M., Schmeing, T. M., Kelley, A. C., and Ramakrishnan, V. (2010) The Mechanism for Activation of GTP Hydrolysis on the Ribosome. *Science 330*, 835−838.
(42) Zhou, J., Lancaster, L., Trakhanov, S., and Noller, H. F. (2012) Crystal structure of release factor RF3 trapped in the GTP state on a rotated conformation of the ribosome. *RNA 18*, 230−240.
(43) Roll-Mecak, A., Cao, C., Dever, T. E., and Burley, S. K. (2000) X-ray structures of the universal translation initiation factor IF2/eIF5B: Conformational changes on GDP and GTP binding. *Cell 103*, 781−792.
(44) Bi, X., Corpina, R. A., and Goldberg, J. (2002) Structure of the Sec23/24-Sar1 pre-budding complex of the COPII vesicle coat. *Nature 419*, 271−277.
(45) Ghosh, A., Praefcke, G. J. K., Renault, L., Wittinghofer, A., and Herrmann, C. (2006) How guanylate-binding proteins achieve assembly-stimulated processive cleavage of GTP to GMP. *Nature 440*, 101−104.
(46) Ismail, S. A., Vetter, I. R., Sot, B., and Wittinghofer, A. (2010) The structure of an Arf-ArfGAP complex reveals a Ca^{2+} regulatory mechanism. *Cell 141*, 812−821.
(47) Leipe, D. D., Wolf, Y. I., Koonin, E. V., and Aravind, L. (2002) Classification and evolution of P-loop GTPases and related ATPases. *J. Mol. Biol. 317*, 41−72.